doi.org/10.26434/chemrxiv.7637081.v2

Bio-Copolyesters of Poly(butylene succinate)(PBS) Containing Long Chain Bio-Based Glycol

Karolina Stępień, Cathrine Miles, Andrew McClain, Ewa Wiśniewska, Peter Sobolewski, Joachim Kohn, Judit E. Puskas, H. Daniel Wagner, Miroslawa El Fray

Submitted date: 22/05/2019 • Posted date: 22/05/2019

Citation information: Stępień, Karolina; Miles, Cathrine; McClain, Andrew; Wiśniewska, Ewa; Sobolewski, Peter; Kohn, Joachim; et al. (2019): Bio-Copolyesters of Poly(butylene succinate)(PBS) Containing Long Chain Bio-Based Glycol. ChemRxiv. Preprint.

Poly(butylene succinate) (PBS) is a thermoplastic and biodegradable polyester characterized by high rigidity due to its high crystallinity. However, the use of long chain biobased monomers to produce segmented copolymers is an effective strategy to tailor the properties of PBS, such as greater flexibility. In this paper, a series of aliphatic bio-copolyesters of poly(butylene succinate-dilinoleic succinate) (PBS-DLS) were successfully synthesized via a direct two-step polycondensation method using a semi-pilot scale reactor for melt polymerization and titanium dioxide/silicon dioxide coprecipitate catalyst (C-94). In this study, the thermal and mechanical properties were investigated and compared, focusing on the effect of varying the amount of biobased dilinoleic diol in the structure. With increasing amount of long chain diol, a decrease in molecular weight, density, and melt flow index was observed. The semicrystalline nature of the copolymers was confirmed using differential scanning calorimetry (DSC) and dynamic mechanical thermal analysis (DMTA) methods. These copolymers exhibit two main transition temperatures and vary in softness and processing flexibility. Furthermore, in the DSC data a linear trend was observed with increasing wt.% of hard PBS segments, which can be described by the Gordon-Taylor equation. Increasing the soft DLS segment content in the copolymer series resulted in an increase in the elastic behavior of the polymers. The broad range of crystallization temperatures and melt flow index values indicates that a polyester library with customizable properties that spans PBS applications has been successfully obtained.

File list (2)

Bio-copolyesters of poly(butylene succinate)(PBS) containing long chain bio-based glycol

Karolina Stępień [†], Catherine Miles [‡], Andrew McClain [§], Ewa Wiśniewska [†], Peter Sobolewski [†], Joachim Kohn [‡], Judit Puskas [§], H. Daniel Wagner [£], Miroslawa El Fray [†,]*

[†] Faculty of Chemical Technology and Engineering, Division of Functional Materials and Biomaterials, West Pomeranian University of Technology, Szczecin, Al. Piastów 45, 71-310 Szczecin, Poland

[‡] The New Jersey Center for Biomaterials, Rutgers, The State University of New Jersey, Piscataway, NJ, 08854, USA

[§] Department of Chemical and Biomolecular Engineering, The University of Akron, Akron, OH, 44325, USA

[£] Department of Materials and Interfaces, Weizmann Institute of Science, Rehovot, 76100, Israel

*corresponding author mirfray@zut.edu.pl

Graphical Abstract

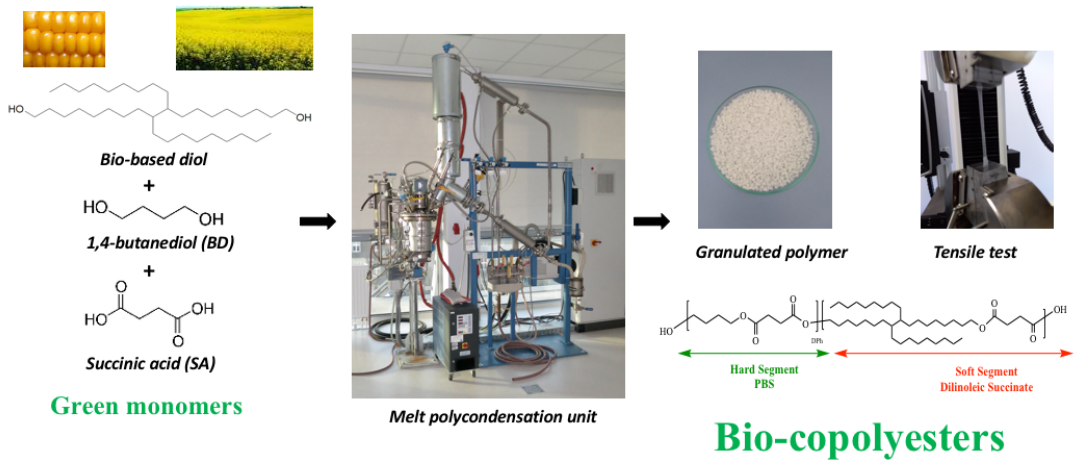

Abstract

Poly(butylene succinate) (PBS) is a thermoplastic and biodegradable polyester characterized by high rigidity due to its high crystallinity. However, the use of long chain biobased monomers to produce segmented copolymers is an effective strategy to tailor the properties of PBS, such as greater flexibility. In this paper, a series of aliphatic bio-copolyesters of poly(butylene succinate-dilinoleic succinate) (PBS-DLS) were successfully synthesized *via* a direct two-step polycondensation method using a semi-pilot scale reactor for melt polymerization and titanium dioxide/silicon dioxide coprecipitate catalyst (C-94). In this study, the thermal and mechanical properties were investigated and compared, focusing on the effect of varying the amount of biobased dilinoleic diol in the structure. With increasing amount of long chain diol, a decrease in molecular weight, density, and melt flow index was observed. The semicrystalline nature of the copolymers was confirmed using differential scanning calorimetry (DSC) and dynamic mechanical thermal analysis (DMTA) methods. These copolymers exhibit two main transition temperatures and vary in softness and processing flexibility. Furthermore, in the DSC data a linear trend was observed with increasing wt.% of hard PBS segments, which can be described by the Gordon-Taylor equation. Increasing the soft DLS segment content in the copolymer series resulted in an increase in the elastic behavior of the polymers. The broad range of crystallization temperatures and melt flow index values indicates that a polyester library with customizable properties that spans PBS applications has been successfully obtained.

KEY WORDS

poly(butylene succinate), polycondensation, titanium dioxide, thermal properties, mechanical tests

INTRODUCTION

For several decades, aliphatic polyesters have been widely investigated for various applications including medicine and food packaging, due to their ability to degrade in a given environment [1–3]. Poly(ε-caprolactone) (PCL)[4], poly(lactic acid) (PLA) and poly(glycolic acid) (PGA) [5], poly(hydroxybutyrate) (PHB) and other polyhydroxyalkanoates (PHA) [6] are among a few of the polymers that are currently in development or on the market for use in biomaterial applications. These materials are characterized by their biodegradability under biological conditions, good biocompatibility, and suitable mechanical properties that match the properties of human tissue [7]. Although these polymers are widely used and well established, there is a constant need for the development of new materials. For example, many of the previously mentioned polymers degrade into acidic byproducts, which can cause an inflammatory response, or have mechanical properties that do not suitably match human soft tissues [1].

Recent research has focused on the synthesis of "green" polymers: biodegradable polymers that are derived from renewable resources, offering much improved sustainability [8–10]. Of particular interest is the aliphatic polyester poly(butylene succinate) (PBS) [11], that was "rediscovered" in the early 90's and commercialized by Mitsubishi Chemicals Corporation and Showa-Denko under trademark Bionolle™. Due to its susceptibility to decomposition, ease of processing, and durability, PBS is widely investigated for use in biomaterials, including tissue engineering [12]. Further, incorporating PBS as a building block in copolymer synthesis is a versatile strategy towards tailoring its properties and obtaining materials with a two-domain crystalline and amorphous structure [13,14]. Therefore, to understand the structure-property relationship of these new materials, it is necessary to study their crystal structures, thermal properties, and mechanical behavior.

To tailor the advantageous properties of PBS for use in various applications, including biomedicine, the amount of PBS introduced during polymer synthesis can be systematically varied, yielding materials that range from soft and rubber-like to stiff and mechanically stable [15–17]. Many examples of copolymers where various glycols or diacids were used can be found in the literature [12]. For example, the addition of a second comonomer in the structure of poly(butylene succinate-*co*-ethylene succinate) P(BS-*co*-ES) [18,19] or poly(butylene succinate-*co*-hexamethylene succinate) P(BS-*co*-HS) [20] decreases the polymer melting temperature. Further work by Cao et al. [18] using differential scanning calorimetry (DSC) demonstrated that the thermal properties and crystallization behavior of PBS copolymers with the second comonomer being ethylene succinate or diethylene succinate strongly depend on the corresponding comonomer composition. Meanwhile, the addition of an amorphous phase changes the degree of polycondensation [21]. Finally, the use of long chain aliphatic biobased diols has seldom been reported, with decamethylene diol as the only found example [16].

In our earlier work, we described a series of PBS copolymers with soft segments consisting of biobased C36 diacid, a dimer of linoleic acid [22]. These copolymers showed two

main transition temperatures and spanned a wide range of softness and processing flexibility. The synthesis was carried out under vacuum at 230 °C using titanium tetrabutoxide (TBT), a classical organometallic catalyst.

Here, we present a new series of aliphatic multiblock copolymers of poly(butylene succinate-dilinoleic succinate) (PBS-DLS) with a long chain biobased glycol, here abbreviated as dilinoleic diol, a dimerization product of C18 linoleic acid. PBS sequences constitute the hard segments and DLS sequences constitute the soft segments. By using the biobased dilinoleic diol, we embrace the sustainability offered by the other monomers (1,4-butanediol, succinic acid) that can be obtained from biomass—entirely biobased PBS is commercially available [9]. Further, the present synthesis uses an alternative catalytic system: a titanium dioxide/silicon dioxide coprecipitate catalyst (C-94) originally developed by Acordis/Akzo Nobel as an alternative to antimony-based catalysts for polyethylene terephthalate (PET) synthesis [23,24]. To our knowledge, we are the only group using this catalyst for PBS synthesis. It offers advantages important over the organometallic TBT catalyst that is typically used for PBS synthesis[12]: 1) as a solid powder, it is a heterogeneous catalyst system, 2) it's hydrolytically stable and does not require distillation before use, and 3) it carries a lower environmental, health, and safety impact than the hazardous TBT [23–25]. These advantages are particularly relevant to PBS and PBS-copolymer synthesis, since water is a by-product of the initial synthesis stage. Meanwhile, reducing toxicity/environmental impact is paramount given the biodegradablity, as well as potential biomedical/biomaterial applications of PBS-based materials. Both the synthesis and properties of this series of PBS-DLS copolymers will be discussed, focusing on the effect of soft segment content containing dilinoleic diol on polymer structure—as determined by spectral analysis—and properties, including thermal, mechanical, and crystallinity.

MATERIALS AND METHODS

Materials

All reagents used were purchased from commercial sources and were used without further purification. The following reagents were used for copolymer synthesis: succinic acid, 99+% purity (Alfa Aesar, Germany), 1,4-butanediol (Merck, Germany), dilinoleic diol - Pripol^{TM} 2033 (Croda, United Kingdom), titanium dioxide/silicon dioxide coprecipitate catalyst C-94 (Huntsman, Germany).

Copolymer Synthesis

A series of copolymers, herein abbreviated as PBS-DLS, were prepared using a two-step synthesis. The synthesis scheme is presented in **Figure 1.** First, 1,4-butanediol and succinic acid were copolymerized at 180 °C in the presence of titanium dioxide/silicon dioxide coprecipitate C-94 catalyst, through an esterification reaction. The reaction was run until 95% of the theoretical amount of water was collected. In the second step, a long hydrocarbon glycol (dilinoleic diol, Pripol^{TM} 2033) and a second aliquot of C-94 catalyst was added to the reaction mixture. Polycondensation started when the pressure was decreased to 0.2-0.4 hPa and

temperature increased to 240 °C. Due to the excellent thermal stability of dilinoleic diol, the process was carried out without the use of thermal stabilizers. The progress of the reaction was monitored by power consumption of the stirrer of the fully automated polycondensation unit (3 L stainless steel reactor, Fourne GmbH, Germany, **Figure 2**).

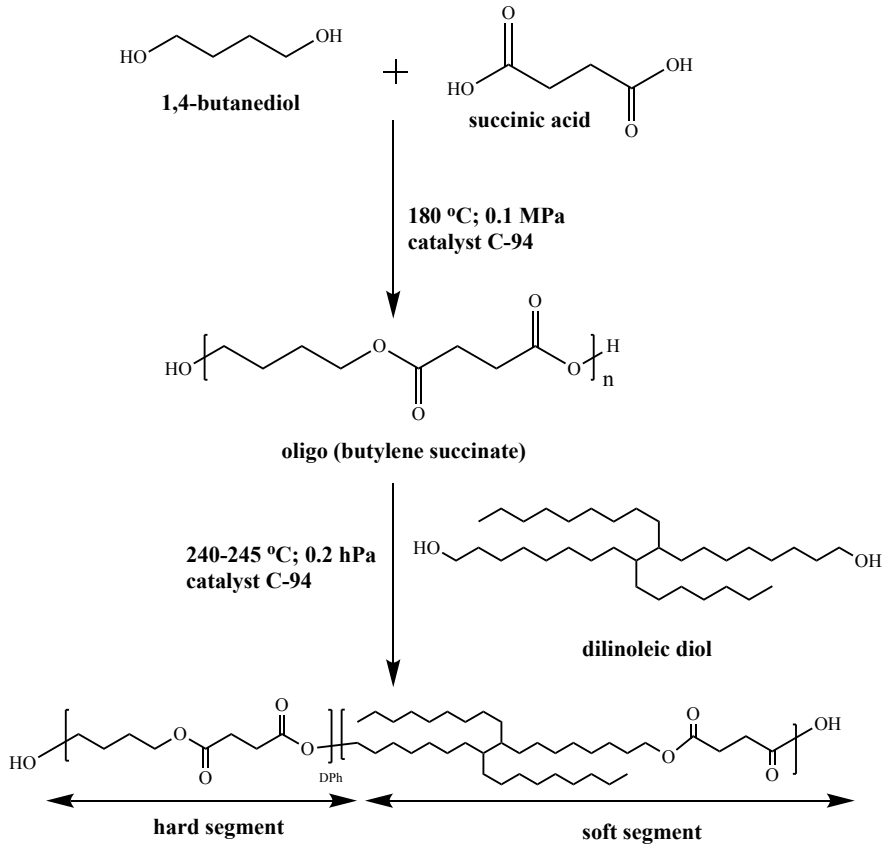

POLY(BUTYLENE SUCCINATE-DILINOLEIC SUCCINATE)

Figure 1. Schematic two-step synthesis of PBS-DLS copolymers.

Using the described synthesis, a series of PBS-DLS multiblock copolymers consisting of 50:50, 60:40, 70:30 and 80:20 wt.% PBS-DLS hard:soft segments were successfully synthesized in 800 g batches. The degree of polycondensation (DP_h) of PBS hard segments was 3.9, 5.8, 9.1 and 15.6, respectively. Additionally, PBS homopolymer (DP_h = 192) was synthesized under analogous conditions (catalyst, temperature, and pressure).

Figure 2. The 3L stainless steel polycondensation unit used for polyester synthesis.

Nuclear Magnetic Resonance (NMR) Spectroscopy

The chemical composition of the copolymers was determined using ^{1}H NMR spectroscopy. The ^{1}H NMR spectra were obtained using a TM Bruker DPX 400 MHz spectrometer using tetramethylsilane (TMS) as an internal reference. A sample of dried polymer, ~5 mg, was dissolved in $CDCl_3$ and 128 scans were collected for ^{1}H NMR at room temperature and a 1 second relaxation time. The molar and weight percent ratios of PBS and DLS were calculated by integrating the respective ^{1}H NMR peaks. To confirm the structural identity of the polymers, ^{13}C NMR was performed using a TM Bruker DPX 400 MHz spectrometer using tetramethylsilane (TMS) as an internal reference. A sample of dried polymer, ~5 mg, was dissolved in $CDCl_3$ and 512 scans were collected at room temperature and a 1 second relaxation time.

Fourier Transform Infrared (FTIR) Spectroscopy

FTIR spectra were collected using a Bruker ALPHA spectrometer with an Attenuated Total Reflectance (ATR) cell between 500 and 4000 cm^{-1} and at 4 cm^{-1} resolution. A sample of dried polymer was placed on the aperture and 32 scans were averaged across the spectral range to improve the signal-to-noise ratio.

Gel Permeation Chromatography/Size Exclusion Chromatography (GPC/SEC)

Qualitative SEC measurements were performed in a set-up consisting of an Agilent 1260 Infinity Isocratic Pump (Agilent Technologies, Santa Clara, CA, USA), a Wyatt OPTILAB T-rEX interferometric refractometer (Wyatt Technology, Santa Barbara, CA, USA), a Wyatt DAWN HELOS-II multi-angle static light scattering detector (MALS) (Wyatt Technology, Santa Barbara, CA, USA) with a built-in dynamic light scattering (DLS) module, an Agilent 1260 Infinity Standard Autosampler (Agilent Technologies, Santa Clara, CA, USA) and 6 StyragelVR columns (HR6, HR5, HR4, HR3, HR1, and H0.5). The columns were thermostatted at 35 °C and tetrahydrofuran (THF), continuously distilled from CaH_2, was used as the mobile phase at a flow rate of 1 mL/min. Prior to the analysis, samples were dissolved in THF (the same employed as mobile phase in the instrument) at 2-3 mg/mL and filtered. The differential refractive index signal was analyzed qualitatively.

Matrix Assisted Laser Desorption/Ionization Time-of-Flight Mass Spectrometry (MALDI-ToF MS)

MALDI-ToF measurements were performed on a Bruker Ultra-Flex III instrument (Bruker Daltonics, Billerica, MA) equipped with a Nd:YAG laser (355 nm) and spectra were acquired in positive reflection mode. Instrumental settings were tuned to parameters that optimized signal intensity and resolution. Samples (10 mg/mL), matrix used (*Trans*-2-[3-(4-*tert*-Butylphenyl)-2-methyl-2-propenylidene] malononitrile) (20 mg/mL), and sodium trifluoroacetate (NaTFA) cationizing agent (10 mg/mL) were dissolved in $CHCl_3$. Matrix and salt were purchased from Sigma-Aldrich (St. Louis, MO). All solvents were purchased from Fischer Scientific (Fairlawn, NJ). The matrix and salt solution were mixed 10:1 (v/v) and approximately 0.5-1.0 μL aliquot was spotted onto a 384-well ground-steel MALDI target plate, followed by deposition of the sample solution and another addition of matrix/salt solution (sandwich method). Calibration was performed using PMMA (M_w = 2,000), sodiated with NaTFA. All data was acquired with Bruker's FlexControl software (v3.3). The mass composition of the copolyesters was determined using equation (1):

$$M = M_{\text{end group}} + \left(n * M_{\text{repeating unit}}\right) + M_{Na^+} \quad (1)$$

where M corresponds to the mass of a polymer, $M_{\text{end group}}$ corresponds to the mass of the end group, n is the number of repeating units, $M_{\text{repeating unit}}$ is the mass of the repeating unit, and M_{Na^+} is the mass of the sodium ion.

Differential Scanning Calorimetry (DSC)

Polymer glass transition temperature (T_g), melting temperature (T_m), and crystallization temperature (T_c) were determined using a TA Instruments DSC Q100. Dried polymer, ~12 mg in weight, was sealed in an aluminum pan. Samples were heated from -90 °C to 200 °C at a rate of 10 °C per minute and then held at 200 °C for 1 min to erase the thermal history of the polymer (first heat cycle). The sample was then cooled to -90 °C and held for 1 minute, then heated again from -90 °C to 200 °C at a rate of 10 °C per minute (second heat cycle). The T_g of the polymers was determined from the second heat cycle as the midpoint of the transition. The crystalline phase content in the hard segments ($X_{c,h}$%) was calculated using equation 2 and the total content of crystalline phase in the polymer ($X_{c,tot}$%) was calculated using equation 3, where W_h is the ratio of the hard PBS segment, ΔH_m is the melting enthalpy of the polymer, and ΔH_m° is the reference of 100% crystalline PBS (110.3 J/g) [26].

$$X_{c,h}\% = W_h * \frac{\Delta H_m}{\Delta H_m^\circ} * 100 \qquad (2)$$

$$X_{c,tot}\% = \frac{X_{c,h}\%}{W_h} \qquad (3)$$

Wide Angle X-Ray Scattering (WAXS)

WAXS analysis of the polymers was carried out using a TUR M62 apparatus with a wide-angle horizontal goniometer using a sealed tube Cu$K\alpha$ x-ray generator of 1.54 Å wavelength with a Ni monochromator. Polymer thin films were used for the measurements. The scan parameters included a Bragg angle (2θ) range of 5-38° and 2 deg/min of goniometer speed, at room temperature. Patterns were analyzed using the Scherrer equation (4) to calculate the average crystallite size for each synthesized polymer [27].

$$D_c = \frac{k\lambda}{\beta \cos\theta} \qquad (4)$$

D_c represents the average crystallite size, k represents the shape factor constant (~1), λ represents the X-ray wavelength (0.154056 nm), β represents the full width at half maximum (FWHM) of the diffraction peak (in radians) and θ represents the measured angle of diffraction. All peaks were normalized to the Bragg angle (2θ) peak of 22.5 of each sample respectively. Jade 7 software was used for data fitting.

Dynamic Mechanical Thermal Analysis (DMTA)

Storage modulus, loss modulus, and tanδ were determined using a TA Instruments DMA Q800 V21.1, based on the temperature ramp method and PN-EN ISO 6721-1:2011 standard. The dimensions of the compression molded samples were ~20 mm in length, ~4 mm in width, and ~300 μm in thickness. The samples were conditioned at 40 °C for 24 h and then heated

from -100 °C to 150 °C at a rate of 1 °C/min under liquid nitrogen gas supply; tests were performed with an amplitude of 10 mm and frequency of 1 Hz.

Mechanical Testing

The Young's modulus, stress at break, strain at break, and elastic recovery were determined using an Instron 3366 testing instrument. Samples for mechanical testing were prepared using a Remi-Plast hot-press instrument (Remi-Plast, Czerwonak, Poland) at 80 Bar pressure and at a temperature 20 °C above the T_m of each copolymer (T_m was determined using a Boetius melting point microscope), see Table 1. Rectangular, dog-bone specimens with dimensions of 20 mm in length, 4 mm in width, and ~300 μm in thickness were prepared using an Endeavour Lab (Dobra, Poland) device. Quasi-static mechanical tests and cyclic loading-unloading tests were performed with wedge action grips characterized by rate capacity of 30 kN, at room temperature. The initial test speed was 1 mm/min from 0.25% until the sample reached 0.5% of the relative elongation. From 0.5% of the relative elongation to the break point, the test speed was 100 mm/min. The cyclic loading-unloading tests were performed under initial 1 MPa preload and after that test speed was 100 mm/min. During the tests, 20 cycles of loading and unloading were performed up to 50% of the initial strain. The value of elastic recovery was determined on the basis of the obtained loops. The cyclic loading has been repeated for the same samples after 48 h of relaxation.

Intrinsic viscosity

The intrinsic viscosity [η] was measured using an Ubbelohde viscometer (K = 0.00347) immersed in a water bath at 25 °C. Polymers were dried for 48 h and dissolved in $CHCl_3$ to obtain a concentration of 0.5 g/100 cm^3. Values were calculated using the Solomon–Ciuta equations [28].

$$\eta = \frac{\sqrt{2(n_w * \ln \eta_r}}{c} \quad (5)$$

$$\eta_w = \boldsymbol{n_r} * \mathbf{1} \quad (6)$$

$$\eta_r = \frac{t_1}{t_o} \quad (7)$$

where:

t_o = average flow time for solvent (s)

t_1 = average flow time for polymer solution (s)

c = concentration of polymer solution (g/100 mL)

Melt Flow Index (MFI)

The MFI was measured according to ISO 1131-1991 (PN-93/C-89069) using a CAEST type CA-MAN-001 at 140 °C and 2.16 kg of load. The MFI was calculated according to equation (8):

$$MFI = \frac{600 * m}{t} \quad (8)$$

where:

m = mass of sample after desired period of time (g)

t = period of time (s)

600 = reference time (10 min = 600 s)

Cytotoxicity Test

To assess cytotoxity of obtained polymers, extracts were prepared and tested *in vitro* according to ISO10993-5 [29]. First, hot-pressed foils of each material (~0.3 mm thick) were cut into 6 cm^2 strips (~200 mg), sterilized with 70% isopropyl alcohol, and triple rinsed with sterile deionized water. Next, each sample (3 per material) was cut into 8–10 fragments, which were placed in a well of a 24-well plate and covered with 2 mL of complete growth media (DMEM containing 10% fetal bovine serum (FBS), 2 mM L-glutamine, 100 U/mL penicillin, and 100 µg/mL streptomycin). The plate was then incubated in a cell culture CO_2 incubator at 37 °C for 24 hours. In parallel, L929 murine fibroblasts were plated at 10,000 cells per well in a 96-well plate. After 24 hours of culture in complete growth media, the media was replaced with 100 µL of each sample extract (4 technical replicates per sample) and the plate was again incubated for 24 hours. Finally, cell viability was assessed using phase contrast microscopy and resazurin viability assay [30]. Briefly, 20 µL of 0.15 mg/mL sterile resazurin stock in PBS was added to each test well and the plate was incubated for 4 hours at 37 °C. Fluorescence (Em: 540, Ex: 590) was measured using BioTek Synergy HTX multifunctional plate reader.

RESULTS AND DISCUSSION

Characterization of chemical structure of PBS-DLS copolymers

A series of polyesters with varying amounts of hard and soft segments were successfully synthesized, as confirmed by ^{1}H NMR and ^{13}C NMR results. ^{1}H NMR spectra of the polyester series are shown in **Figure 3.** All spectra were normalized to the signal appearing at δ^1H = 2.62 ppm (c) which corresponds to the CH_2 protons in the succinic acid segment. Final wt.% PBS and DLS segments were calculated using δ^1H = 1.71 ppm (d) and δ^1H = 0.87 ppm (g) respectively.

The signals characteristic for the hard PBS segment (peaks (a) and (d) in **Figure 3**) are: δ^1H = 4.12 ppm from the four protons adjacent to the oxygen on butanediol (a), δ^1H = 2.62 ppm (c), and δ^1H = 1.71 ppm from the four internal protons on butanediol (d). The signals characteristic for the soft DLS segment (peaks (b), (e), (f), and (g) in **Figure 3**) are: δ^1H = 4.12 ppm from the four protons adjacent to the oxygen on dilinoleic diol (b), δ^1H = 1.61 ppm from the two central CH protons on dilinoleic diol (e), δ^1H = 1.25 ppm from the 60 internal protons on dilinoleic diol (f), and δ^1H = 1.71 ppm from the six terminal protons on dilinoleic diol (g). Peak (c) is found in both the soft and hard polymer segments. The exact chemical composition was calculated using the relative peak intensities of the protons arising from PBS component, peak (d), and from the DLS component, peak (g).

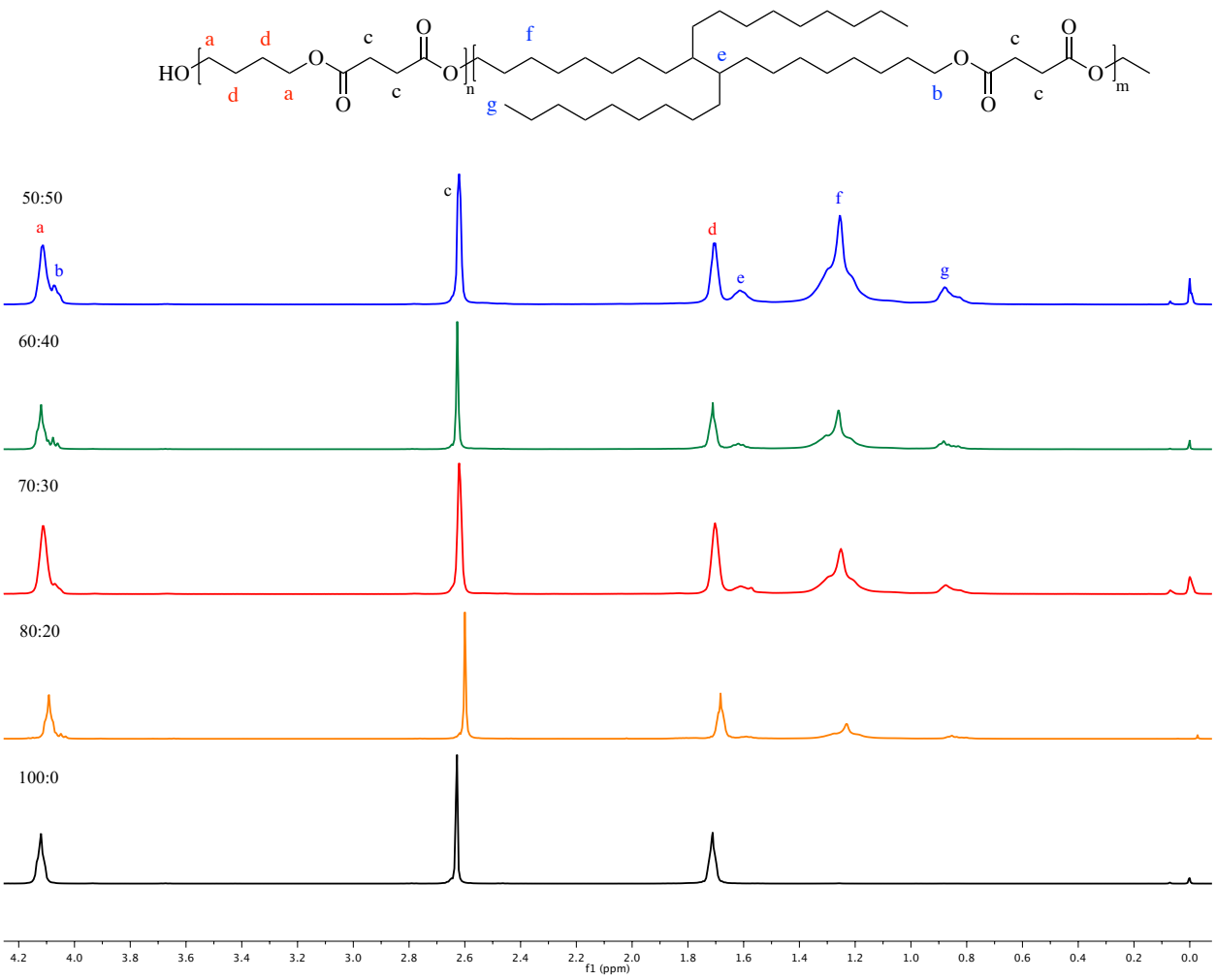

Figure 3. ^{1}H NMR spectra of the synthesized series of poly(butylene succinate-co-dilinoleic succinate) copolyesters. In depicted chemical structure (top), peak (c) indicates protons found in both the PBS and DLS segments, peaks (a) and (d) refer to protons found only in the PBS segment, and peaks (b), (e), (f), and (g) refer to protons found only in the DLS segment.

An increase in the soft DLS segments is observed by the increase in peak (e), peak (f), and peak (g) intensities relative to peak (d). An increase in the shoulder peak (b) correlates to an increase in the protons found next to the ester in the DLS segments, again confirming an increase in the soft DLS segments with increasing DLS feed during the synthesis process. The final polymer compositions (PBS-DLS wt.% ratios) as determined from ^{1}H NMR were: 100:0, 73:27, 66:34, 51:49, and 46:54, as compared to the initial monomer feeds of 100:0, 80:20, 70:30, 60:40, 50:50, respectively.

To further confirm the chemical structures of the polymer series, FTIR-ATR analysis was performed (**Figure 4**). The main characteristic peaks of the polymers are the two peaks at 2925 and 2850 cm^{-1} due to the methylene CH_2 stretching of the soft DLS segments. The peak at 1710 cm^{-1} is due to the carbonyl C=O stretch and the peak at 1150 cm^{-1} and the shoulder at 1180 cm^{-1} are from the ester C-O-C stretch. The fingerprint region between 1000 and 500 cm^{-1} is mostly

composed of the aliphatic C-H and C-C in-plane and out-of-plane bending. All spectra were normalized to the peak at 1700 cm^{-1}. The introduction of soft DLS segments resulted in an increase in the CH_3 alkane C-H stretching peak at 2925 cm^{-1} and an increase in the CH_2 alkane C-H stretching peak at 2850 cm^{-1}. No significant differences in the fingerprint region were observed in the copolymer series. The main conclusions that can be drawn from FTIR spectra are that the expected functional groups are present in the polymers.

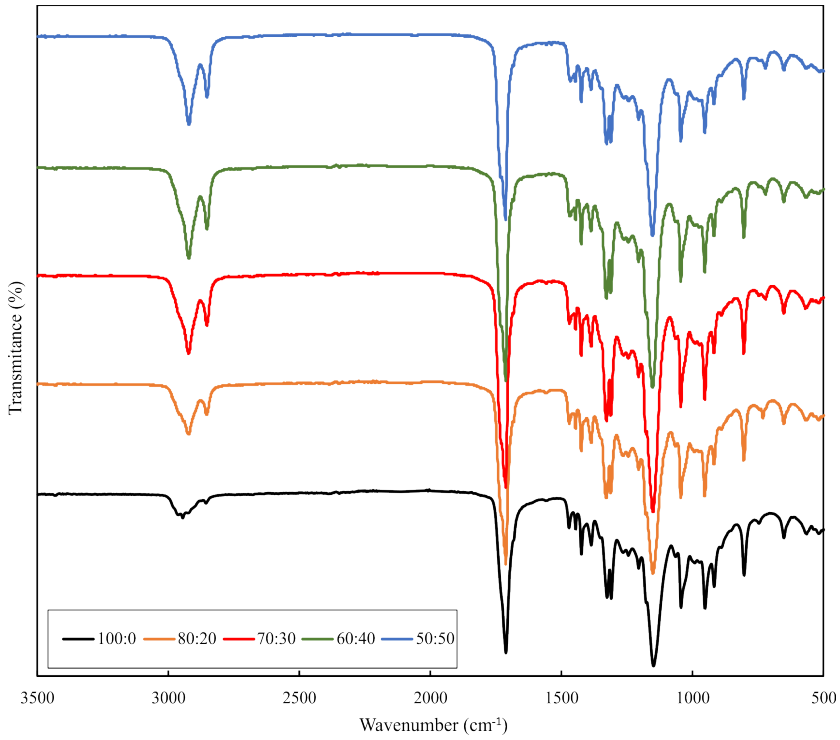

Figure 4. FTIR-ATR spectra (normalized to the peak at 1700 cm^{-1}) of the PBS-DLS copolymer series and PBS homopolymer.

The molecular weight, intrinsic viscosity, and density of the polymers were evaluated to better understand the effect of the hard to soft segment ratio on polymer properties. The results are summarized in **Table 1**. By increasing the amount of soft DLS segments in the PBS-DLS copolymers, a lower degree of polycondensation was obtained. This is in agreement with the molecular number values of the polymers, because the DLS segment has a higher molecular weight than the hard PBS segment. The results in **Table 1** indicate that increasing the wt.% of the soft DLS segment up to 70 wt.% raises the intrinsic viscosity (η) up to 1.182 dL/g. At higher DLS content, the increase in dilinoleic diol causes a decrease in η: the copolymer with a PBS to DLS wt.% ratio of 80:20 exhibited a η value of 0.996 dL/g. The analysis of η suggests that the DP_h does not have a linear influence on η. The MFI value is useful for drawing conclusions regarding polymer molecular weight and polymer composition. The higher the MFI value, the lower the molecular weight and the shorter the monomer lengths, making it easier for the monomer units to slide past one another. By decreasing the amount of smaller PBS segments in

the polymer, the chains take longer to slip past one another during heating. Therefore PBS homopolymer has the highest MFI value while poly(PBS-*co*-50 wt.%-DLS) has the lowest MFI value.

Table 1. Sample designation, polymer composition, and select properties of the PBS-DLS copolymer series.

Sample	PBS W_h (wt.%)[a]	DLS W_s (wt.%)[a]	DP_h[b]	M_n (g/mol)[c]	η (dL/g)[d]	d (dL/g)[e]	MFI (g /10 min)[f]
PBS	100	0	192	53,700	0.865	1.26	18.3 ± 0.4
PBS-DLS 80:20	80 (73)	20 (27)	15.6	112,400	0.996	1.15	4.6 ± 0.1
PBS-DLS 70:30	70 (66)	30 (34)	9.1	38,450	1.182	1.14	2.6 ± 0.2
PBS-DLS 60:40	60 (51)	40 (49)	5.8	35,770	1.114	1.12	1.8 ± 0.2
PBS-DLS 50:50	50 (46)	50 (54)	3.9	17,420	0.924	0.98	<< 1

[a] Theoretical wt.% values are shown, actual wt.% values as calculated from ^{1}H NMR are shown in parenthesis. [b] Degree of polycondensation (DP_h). [c] Average molecular weight (M_n), calculated from GPC/SEC. [d] Intrinsic viscosity (η). [e] Polymer density (d). [f] Melt flow index (MFI).

Using mass spectrometry, the low molar mass fraction of co-monomers of the PBS-DLS that differ in their hard to soft segment ratios were studied for incorporation of segments. Representative samples of 70:30 and 50:50 wt.% were selected for analysis. The following polymer naming scheme is used for the MALDI-ToF/MS data: a subscript number indicates the incorporation of segments, with A representing a PBS segment and B representing a DLS segment. For example, A_nB_1 represents the incorporation of one segment of PBS to the polymer and A_nB_0 represents the PBS homopolymer. In the 70:30 sample, two major distributions were present, one representative of the PBS homopolymer (*m/z*: 1055.59, 1227.67, 13999.79, 1571.89, 1743.99, and 1916.09) and the other representative of the incorporation of one soft segment into the polymer, A_nB_1 (*m/z*: 1157.96,1330.06, 1502.16, 1674.26, 1846.36, and 2018.46), **Figure 5**. There are no minor distributions in the low molecular weight region 1000-1500 *m/z*. Interestingly, this spectrum contains two distinct mass to charge ratios (*m/z*: 1199.85 and 1371.99), confirming the presence of an end group with a mass of 28 Da. Exact reason for presence of a C-OH end group seen at only two mass to charge ratios is unknown, but may represent ionization scission of a hard segment repeat unit or contamination.

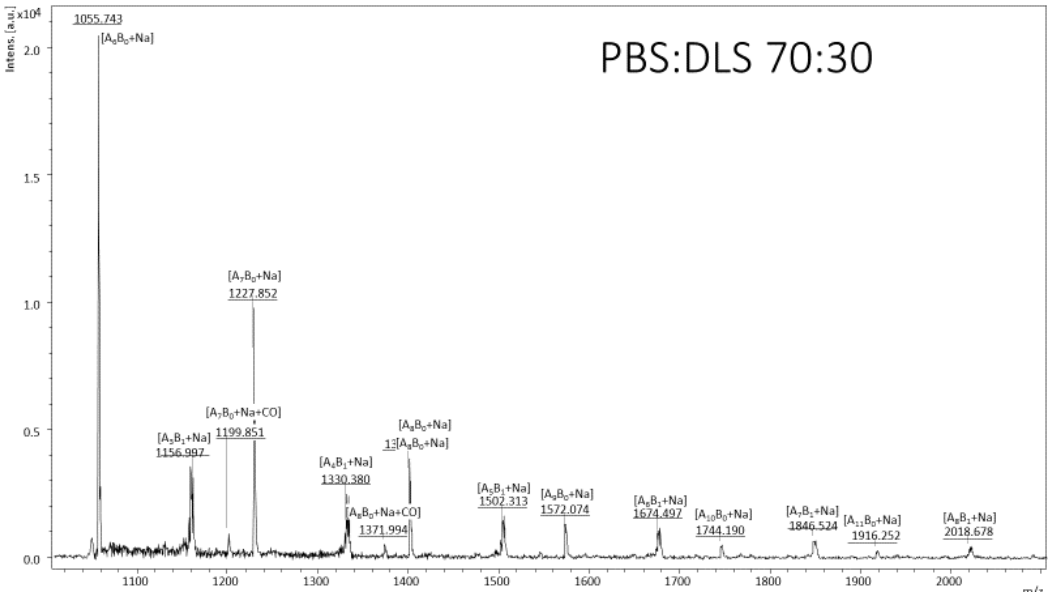

Figure 5. MALDI-ToF/MS spectrum of PBS-DLS 70:30 with two distributions of PBS homopolymer (*m/z* :1055.59, 1227.67, 13999.79, 1571.89, 1743.99, and 1916.09*)*, and the other representative of the incorporation of one soft segment into the polymer, A_nB_1 (*m/z*: 1157.96,1330.06, 1502.16, 1674.26, 1846.36, and 2018.46).

MALDI-ToF spectrum for the 50:50 copolymer, **Figure 6**, had all previously described distributions present (homopolymer: *m/z*: 1056.25,1228.47, and 1400.68; A_nB_1: *m/z*: 1158.66, 1330.87,1502.07, 1674.27, 1846.49, 2018.46, and 2190.86) along with a new distribution that confirmed the presence of an A_nB_2 polymer unit (*m/z*: 1432.43,1604.53, 1776.63, 1948.73, 2120.83, and 2292.93), where two soft segment units were found to be incorporated. By increasing the amount of soft segment added during the reaction process, an increase in incorporation was also observed. It seems that with increasing long chain hydrocarbon diol concentration there are more distributions present with a higher number of soft segments incorporated. Ends groups were not seen in any of these spectra and can be assumed to be equal to the butylene-succinate segment as seen with the ^{1}H NMR and ^{13}C NMR low intensity signals for all samples. It may be expected that with increasing DLA-OH content and therefore OH-end groups, there is a higher likelihood for coupling with the particles of a catalyst and hence, increased incorporation with PBS segments.

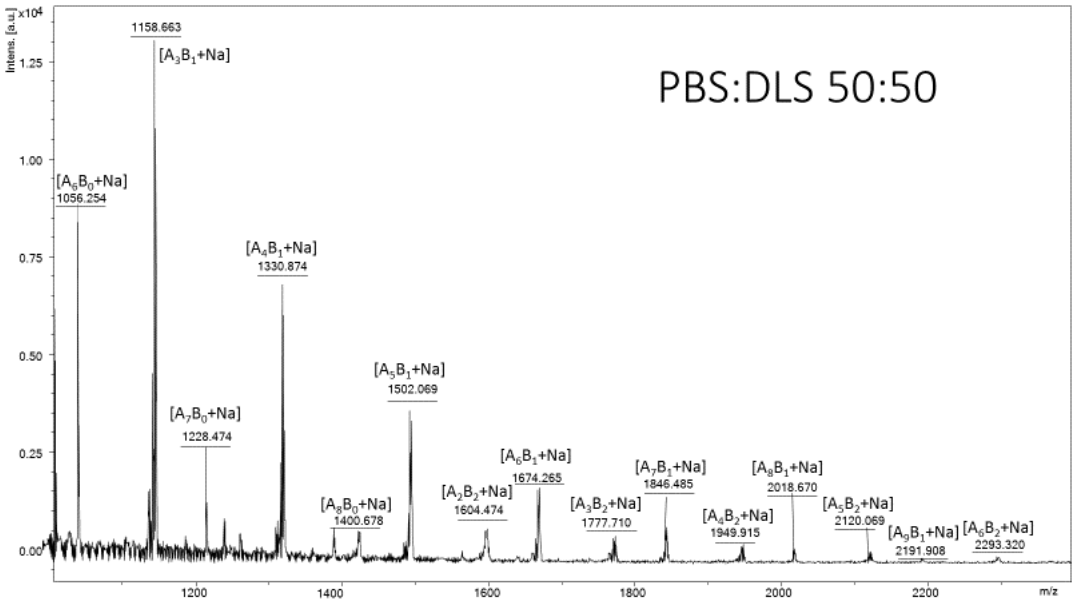

Figure 6. MALDI-ToF/MS spectrum of PBS-DLS 50:50 copolymer including all distributions present in the 70:30 polymer (homopolymer: *m/z*: 1056.25,1228.47, 1400.68; A_nB_1: *m/z*: 1158.66, 1330.87,1502.07, 1674.27, 1846.49, 2018.46, and 2190.86) in addition to a new distribution that confirmed the presence of an A_nB_2 polymer unit (*m/z*: 1432.43,1604.53, 1776.63, 1948.73, 2120.83, and 2292.93).

Thermal properties of PBS-DLS copolymers

All of the copolymers in the library exhibit a melting temperature (T_m) between 88 °C and 115 °C, indicating that they are semicrystalline materials. **Figure 7** shows the DSC traces of the copolymer series and explores the trend in thermal properties with polymer composition.

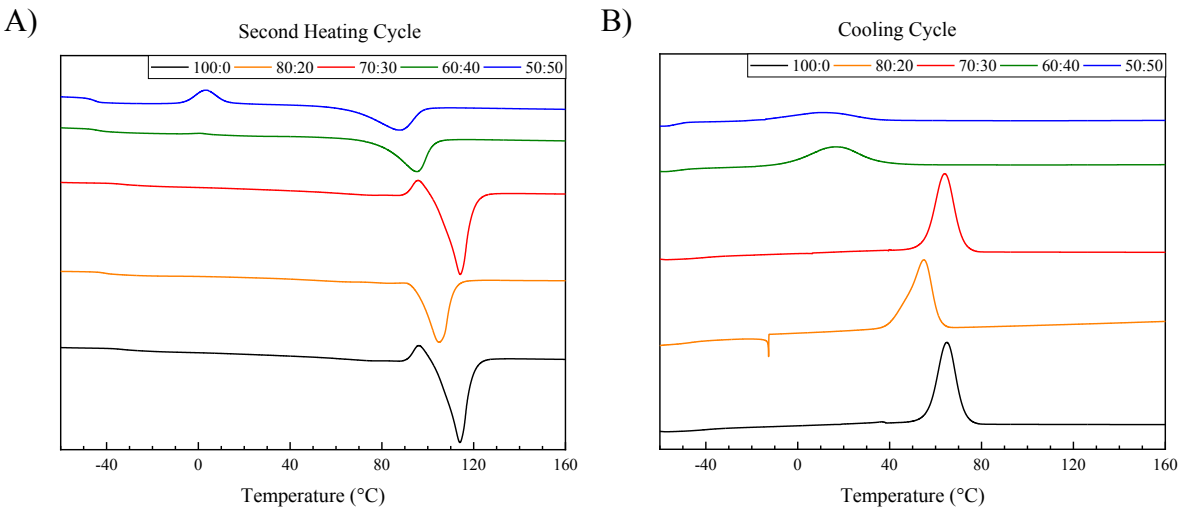

Figure 7. DSC thermograms. (A) second heating cycle of the PBS-DLS copolyester series. (B) cooling cycle of the PBS-DLS copolyester series.

It can be observed that increasing the amount of soft DLS segment resulted in a decrease in melting temperature. This can be attributed to the long aliphatic chains of the DLS segments having lower thermal properties due to their amorphous nature than the more rigid PBS segments. PBS-DLS 60:40 and PBS-DLS 50:50 have a significantly lower melting temperature than materials containing higher amount of crystallizable hard segments of DLS. Further, by increasing the amount of the soft segments, the polymer begins to lose its semicrystallinity, as seen by broadened melting peaks and lower change in melting enthalpy (ΔH_m) values. Table 2 summarizes the thermal properties of the copolymer series. An interesting relationship has been observed for the changes in T_g, T_m, and T_c as the function of PBS hard segment content (**Figure 8**).

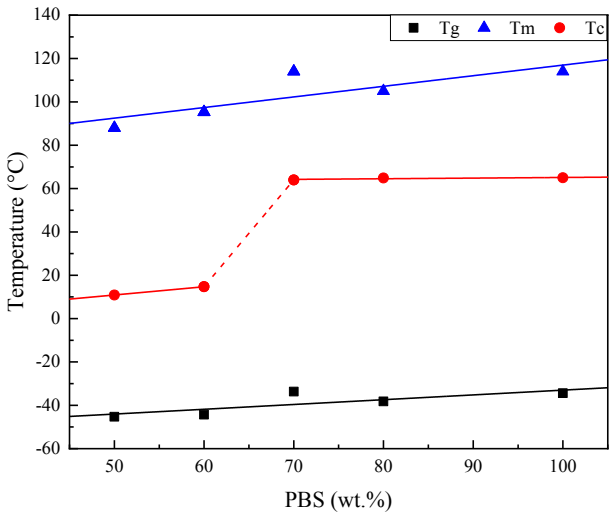

Figure 8. The relationship between the phase transition temperatures, T_g, T_m, and T_c as a function of hard segment content in the PBS-DLS copolyester series.

The T_g traces can be described by the Gordon-Taylor equation[31]:

$$T_g \approx \left[\omega_1 * T_{g,1} + K * \omega_2 * T_{g,2}\right] / \left[\omega_1 + K * \omega_2\right] \qquad (9)$$

where ω_1 and ω_2 is the weight fraction of component 1 and 2 and K is the arbitrary fitting parameter, and follow a linear trend with increasing wt.% of hard PBS segments. This can be attributed to the long aliphatic chains of the DLS segments having lower thermal properties, due to their amorphous phase, than the more rigid PBS segments. There is a marked change in the T_m and T_c of the copolymer series between 60-70 wt.% PBS, as seen in the dotted line region in **Figure 8**. We hypothesize that this is due to the stacking of the polymer chains. At high PBS content, the polymer forms aligned sheets (**Figure 9a**) that stack neatly and contain intramolecular and intermolecular interactions. With an increase in the flexible DLS segment, the

polymer has more flexibility, allowing it to fold in on itself (**Figure 9b**). This creates smaller folded regions that are not able to stack as close together, due to the side chains of the DLS monomer reducing the intermolecular interactions in the structure. This is also seen in the WAXS data, where a loss of crystallinity is observed with increasing the DLS segment. With less intermolecular interactions, the polymer requires less energy to melt and crystallize, than it would if the polymer were stacked closely together and needed to overcome more intra- and intermolecular combined forces.

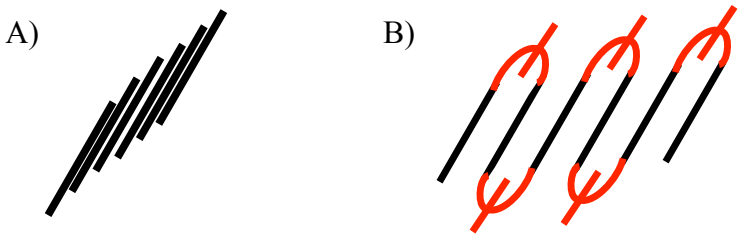

Figure 9. Schematic representation of PBS sheets (A) stacking closely together and PBS-DLS self-folding (B). (black = PBS, red = DLS).

Table 2. DSC and DMTA results for the PBS-DLS copolyester series.

Sample	W_h:W_s	ΔH_m (J/g)	T_m (°C)	T_g (°C)	T_c (°C)	T_{cc} (°C)	$X_{c,h}$ (%)	$X_{c,tot}$ (%)	T_g (E" max) (°C)	T_g (tan δ) (°C)
PBS	100:0	54.2	114.0	-34.4	65.0	-	49.1	49.1	-28.6	-22.1
PBS-DLS 80:20	80:20	53.0	105.0	-38.2	64.9	-	38.4	48.1	-36.3	-29.4
PBS-DLS 70:30	70:30	53.9	114.0	-33.7	64.0	-	34.2	48.9	-41.2	-40.1
PBS-DLS 60:40	60:40	41.6	95.3	-44.3	15.7	2.0	22.6	37.7	-42.7	-39.4
PBS-DLS 50:50	50:50	37.3	88.0	-45.3	10.9	3.6	16.9	33.8	-42.5	-41.6

Melting enthalpy of the hard segments (ΔH_m); melting temperature (T_m); glass transition temperature (T_g); crystallization temperature (T_c); cold crystallization temperature (T_{cc}); crystalline phase content in the hard segment phase ($X_{c,h}$) calculated using equation 2; and total crystalline phase content in the polymer ($X_{c,tot}$) calculated using equation 3. Both $X_{c,h}$ and $X_{c,tot}$ were calculated using the actual W_h segment as determined via ^1H NMR

Structural characteristics with WAXS analysis

The polymer thin films were analyzed using WAXS (**Figure 10**). It can be seen that PBS exhibits crystalline attributes at 2θ = 19.3°, 21.8°, 22.8° and 29.3°, indicating the formation of monoclinic crystals with unit cell parameters of (020), (021), (110) and (111), respectively. Interestingly, the presence of pronounced bell-shape baselines can be observed due to the

presence of an amorphous region. After introducing DLS soft segments an increase in the peak at 19.3° 2θ for copolymer compositions PBS-DLS 80:20 and PBS-DLS 70:30 can be observed. Likewise, the intensity of the 21.8° peak also increases for these copolymers, indicating the ability to crystallize in the PBS crystal cells. Further increase of the amount of DLS soft segments (copolymers PBS-DLS 60:40 and PBS-DLS 50:50) yields peaks of lower intensity, indicating reduced crystallinity compared.

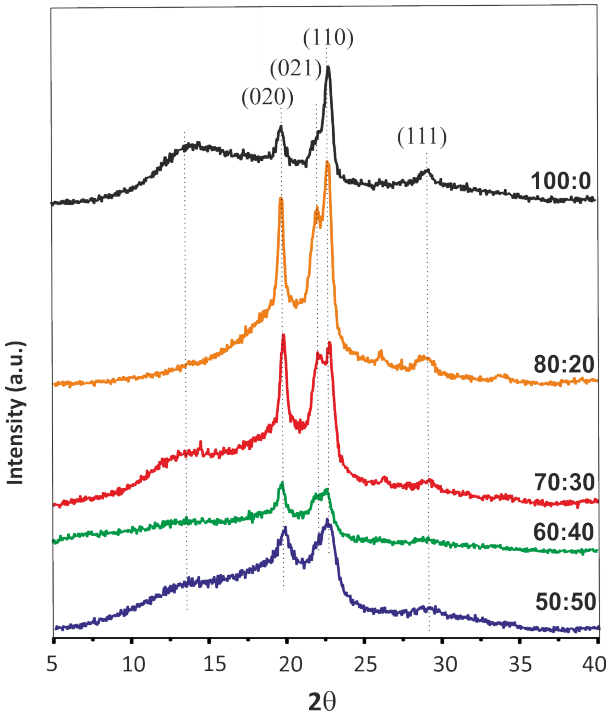

Figure 10. WAXS spectroscopy results of PBS and PBS-DSL copolyester series.

Overall, the copolymers appeared to be less crystalline than PBS homopolymer, consistent with the lower crystallinity degree determined by calorimetric analysis (**Table 2**). It can be concluded that these copolyesters comprising two different segments show different crystalline structures and crystal forms, thus affecting polymer properties, including susceptibility to degradation. Indeed, in earlier work where two PBS-DLS copolyesters were synthesized using enzyme as the catalyst, different spherulitic morphology was observed after degradation [32].

Thermomechanical analysis of PBS-DLS copolymers

Dynamic mechanical analysis of the copolymer series, shown in **Figure 11,** shows a trend between higher DLS segment composition and a loss in polymer storage modulus (E'). A similar trend was observed for the loss modulus (E"). This indicates that increasing the soft DLS segment results in an increase in the elastic behavior of the polymer. This was expected, because PBS is a shorter and stiffer segment, as compared to the long aliphatic DLS monomer unit. The ratio of the loss modulus to the storage modulus (tan δ) measures the dissipation of energy in the material under cyclic loading—it is also called damping. We observed a general trend of higher

damping with increasing DLS composition. This suggests that the PBS homopolymer is the worst at absorbing energy with increasing temperature whereas the PBS-DLS 50:50 copolymer absorbs the most energy with increasing temperature. This is in agreement with the calculated glass transition temperature values of the copolymer series, which show a correlation between decreasing the DLS segment with an increase in the glass transition temperature. The peak damping value follows the same trend as the glass transition temperatures.

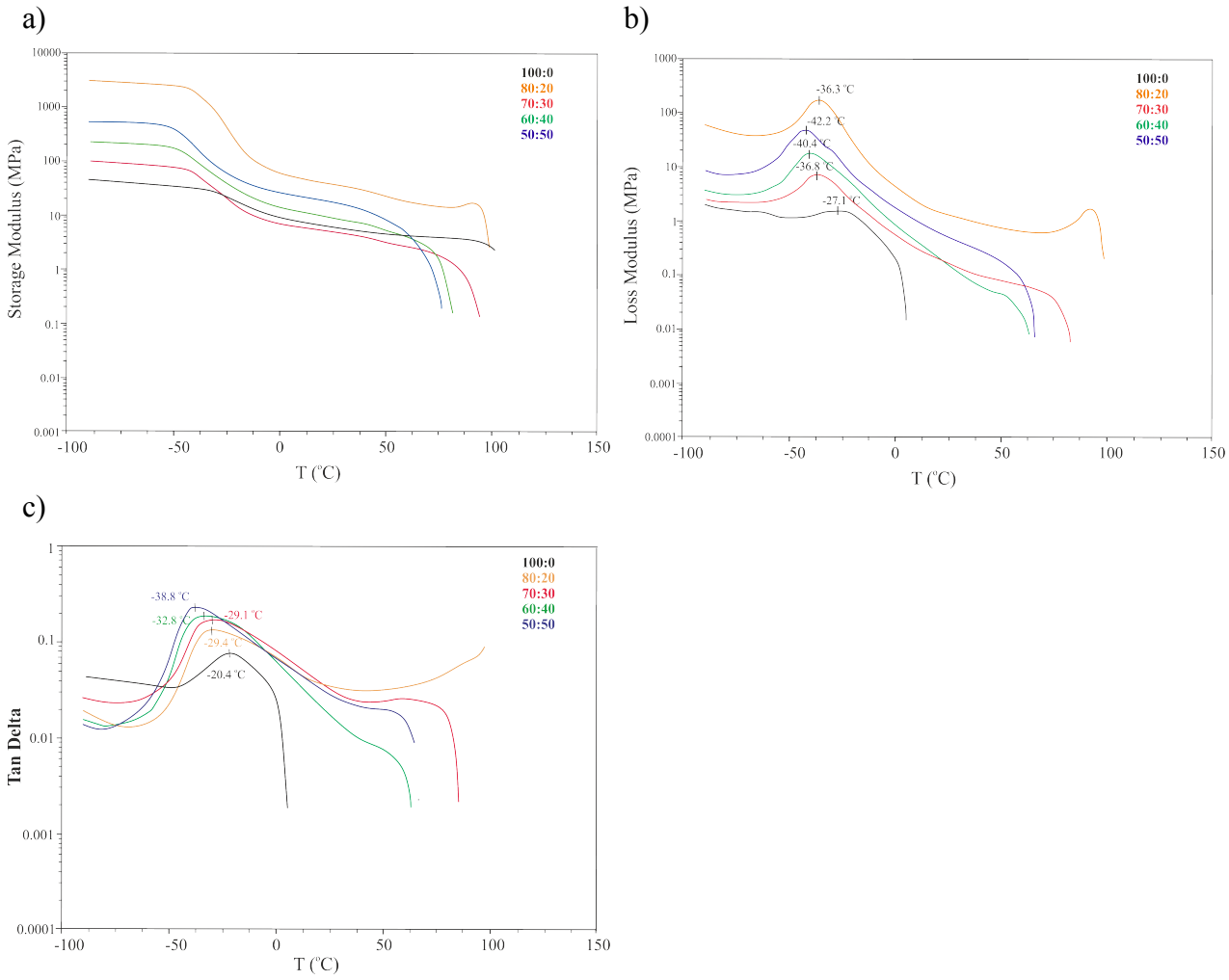

Figure 11. The effect of polymer composition on dynamic mechanical properties: (A) storage modulus (log E′), (B) loss modulus (log E″), (C) damping (log tan δ); PBS (wt.%): (1) 50, (2) 60, (3) 70, (4) 80, (5) 100.

Mechanical characteristics

The mechanical properties of the series of copolyesters and PBS are illustrated by stress-strain curves (**Figure 12**) and the corresponding data (elastic modulus, E; stress at yield point, σ_y; elongation at break, ε_b; and stress at break, σ_b) are summarized in **Table 3**. Cyclic testing was performed to determine the elastic recovery after 20 cycles of deformation ($e_{rec.}$) and elastic

recovery for the same samples after they were allowed to relax for 48 hours ($e_{rec.48}$). The shape of the stress-strain curves for the PBS-DLS copolymers is typical for semi-crystalline, thermoplastic elastomers while the PBS homopolymer exhibits relatively brittle failure at a stress of 31 MPa and elongation of 28%, consistent with prior literature [12].

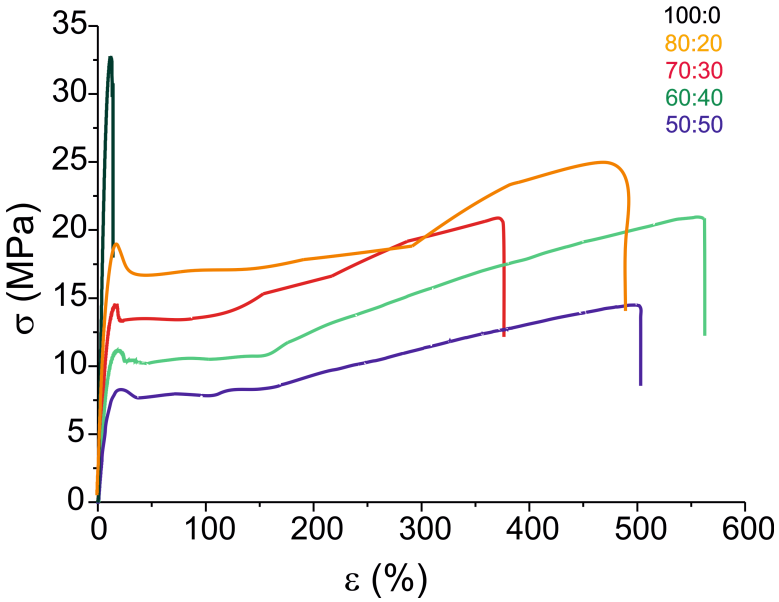

Figure 12. Stress-strain curves for PBS-DLS copolyesters and PBS homopolymer.

As seen in **Table 3**, all materials exhibit a yield point; however, less pronounced yielding can be observed for PBS-DLS 50:50. The amount of hard segments controls the stress at yield point and it becomes sharper (more pronounced) with increasing PBS concentration. The soft segments contribute to the elasticity of the copolymers: the highest strain values were recorded for PBS-DLS 60:40 and PBS-DLS 50:50. At lower soft segment content (increase of PBS hard segments), elongation at break decreases for PBS-DLS 70:30, but an unexpected change of enhanced elasticity and simultaneous increase of yield strain and stress at break was observed for PBS-DLS 80:20. This can be attributed to highest Mn, a different crystalline structure, and highest crystallinity as demonstrated by WAXS data and due to pronounced drawing and orientation zone of the crystalline fibrils demonstrated by long necking zone. The stress-strain curve shows very pronounced strain hardening due to accelerated crystallization and formation of fibrillar crystals [33]. Overall, the decrease in modulus and tensile strength with increasing DLS soft segment content is attributed to a decrease in percent crystallinity (from 48.1% for PBS-DLS 80:20 to 33.8% for PBS-DLS 50:50). However, the higher content of DLS units yielded materials with excellent elasticity, exceeding 400% (in a range from 443 to 585%).

Table 3 Mechanical characterization data of PBS and PBS-DLS multiblock copolymers

Polymer (%)	E (MPa)	σ_y (MPa)	σ_b (MPa)	ε_b (%)	$e_{rec.}$ (%)	$e_{rec.\ 48}$ (%)	σ@50%	σ@50% after 48h
PBS	503 ± 25	32 ± 2.3	31.0 ± 2.0	28 ± 1	-	-	-	-
PBS-DLS 80:20	219 ± 9	18 ± 1.9	28.0 ± 4.2	583 ± 142	40	45	17.5	32.8
PBS-DLS 70:30	171 ± 17	14 ± 0.8	23.0 ± 6.7	443 ± 218	48	59	11.8	25.1
PBS-DLS 60:40	145 ± 11	11 ± 1.2	20.0 ± 2.8	527 ± 128	56	67	9.7	19.7
PBS-DLS 50:50	80 ± 4	8 ± 1.3	13.0 ± 1.0	517 ± 37	73	82	7.4	11.8

Therefore, it was important to investigate their elastomeric properties under cyclic loading-unloading. As can be seen from **Figure 13**, the loading-unloading patterns demonstrate high elasticity, with a recovery dependent on the amount of soft segment content: for PBS-DLS copolymer 50:50 the elastic recovery was 73%, as compared to 48% for copolymer 70:30. It can also be noticed that after the first cycle, the macromolecules are being reoriented and crystallized during straining; therefore, starting from the second cycle, the loading-unloading curves show a build-up of overlapping cyclic loops with very low hysteresis. In order to confirm that cyclic loading is reorganizing the crystalline structure of copolyesters, the tested samples were allowed to relax for 48 hours and then the cycling loading was repeated for 20 cycles. Interestingly, it was observed that the crystal orientation enhances maximum stress at 50% elongation and a greater increase was observed for materials containing the highest amount of crystalline phase, 80 and 70 wt.% PBS, respectively (Table 4), where the yield point can be noticed after the first cycle (**Figure 13**).

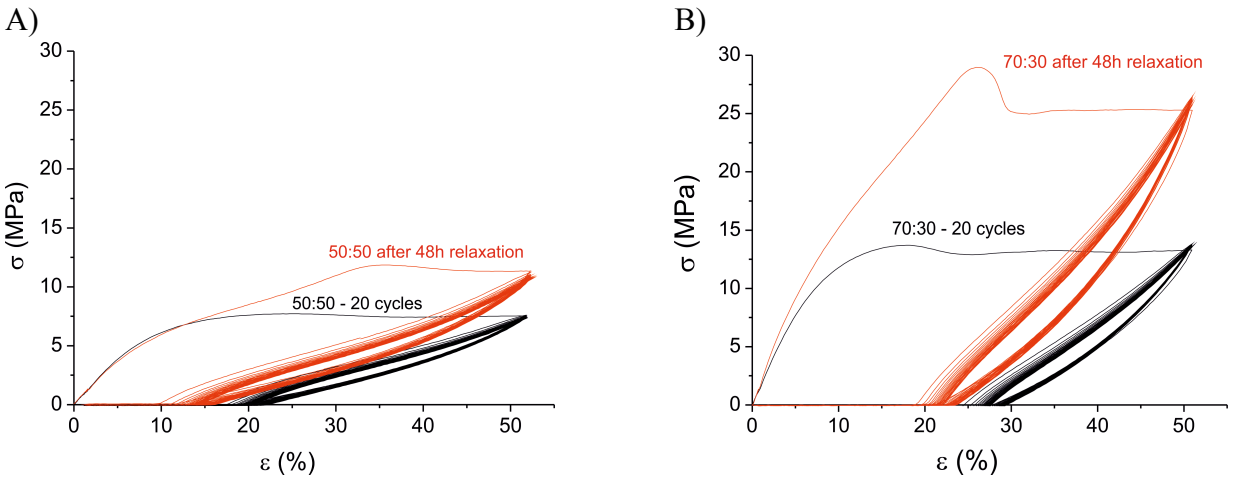

Figure 13. Hysteresis behavior of (A) PBS-DLS 50:50 and (B) PBS-DLS 70:30 copolymers upon cyclic loading for 20 cycles, and further measurements of cycled samples after relaxation for 48 h.

Cytotoxicity Test

A preliminary assessment of the cytotoxicity of the obtained polymers was conducted by testing the effect of extracts on L929 murine fibroblasts *in vitro,* in accordance with ISO10993-5 [29]. After 24 hours of incubation with extracts, the cells were inspected using phase contrast microscopy. For all of the tested materials, a nearly confluent monolayer of cells was observed (**Figure 14**) that was visually similar to that of the sham extract control—no evidence of morphological changes or cell death were observed. Consistent with the microscopic observations, the resasurin viability assay indicated that for all of the copolyesters tested, cell viability was 100% of the sham extract control. Thus, no cytotoxicity effect was observed, indicating that no toxic compounds leached out from the materials, as may be expected given the use of the non-toxic monomers and non-hazardous C-94 catalyst.

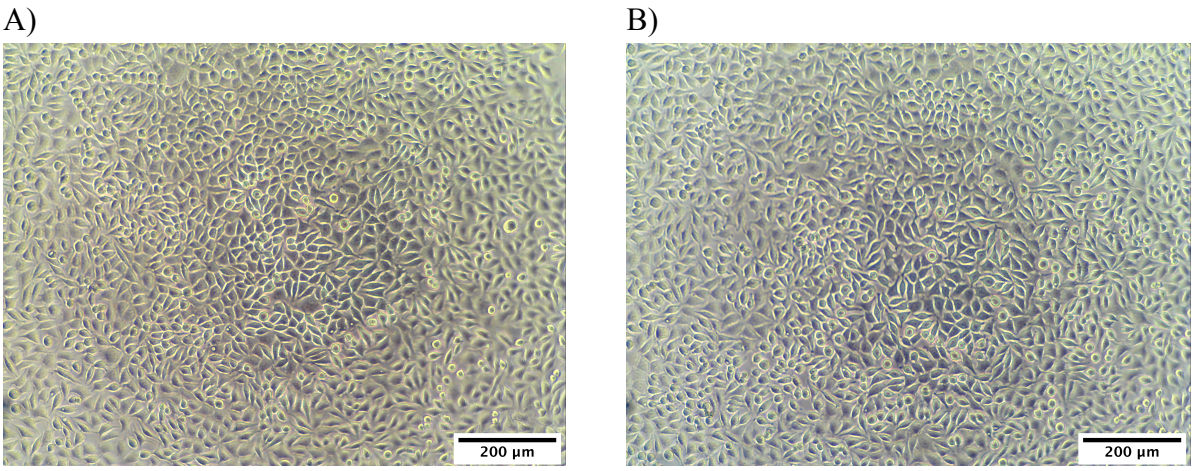

Figure 14. Representative phase contrast micrographs of L929 murine fibroblasts exposed to extracts of (A) PBS-DLS 70:30 and (B) negative control.

Conclusions

A novel series of aliphatic PBS copolymers containing long chain biobased glycol as soft segments was successfully synthesized using a two-step polycondensation technique, with titanium dioxide/silicon dioxide coprecipitate catalyst (C-94). While a number of catalysts have been used for PBS synthesis [34], to our knowledge we are the only group utilizing the C-94 catalyst. The molecular weight and actual composition wt % of our obtained polymers was calculated using GPC and ^{1}H NMR, respectively. For the case of the PBS homopolymer, in comparison to polymer synthesized with the typically-used tetrabutoxy titanate (TBT) catalyst [34], we obtained somewhat higher M_n despite similar reaction conditions, making the use of the hydrolytically-stable and less hazardous C-94 catalyst a clear benefit. Looking at the PBS-DLS copolymers, the molecular weight of the copolymers decreased substantially with increasing soft DLS segment incorporation. The intrinsic viscosity and the degree of polycondensation were both measured to discover that the degree of polycondensation did not have a linear influence on the intrinsic viscosity number. It was confirmed that more PBS segments present in the copolymer resulted in a higher melt flow index. The copolymer series was further characterized

using DSC and WAXS to understand the thermal properties and crystal structure of the polymers. It was observed that all materials synthesized were semicrystalline in nature. The higher concentration of DLS monomer present in the copolymer composition, the lower the melting temperature and the polymer began to lose its crystalline structure. The glass transition temperature of the series can be described by the Gordon-Taylor equation and with increasing wt.% of PBS follows a linear increase in temperature. A significant change in the crystallinity temperatures was observed between 60-70 wt.% PBS, which can be explained using intra- and intermolecular forces present in the different polymers. Mechanical studies showed a correlation between increasing DLS segment with a more elastic and a lower damping effect of the polymer. Finally, *in vitro* cell culture tests of extracts indicate that the synthesized materials are free of toxic leachables. The synthesis and characterization of this new bio-copolyester series has given insight into the many relationships between the amount of hard and soft segment present with respect to both physical and chemical properties which can be tuned for various bio-applications.

AUTHOR INFORMATION

Corresponding Authors

*E-mail: mirfray@zut.edu.pl

ORCID

Miroslawa El Fray: 0000-0002-2474-3517

Author Contributions

The manuscript was written through contributions of all authors.

All authors have given approval to the final version of the manuscript.

Notes

The authors declare no competing financial interest.

ACKNOWLEDGEMENTS

This work is financially supported by National Science Centre, Poland, under the HARMONIA scheme (agreement No. UMO-2014/14/M/ST8/00610). MSc Marcin Michoń is acknowledged for experimental assistance in mechanical tests.

REFERENCES

1. Manavitehrani, I.; Fathi, A.; Badr, H.; Daly, S.; Negahi Shirazi, A.; Dehghani, F. Biomedical Applications of Biodegradable Polyesters. *Polymers (Basel).* **2016**, *8*, 20, doi:10.3390/polym8010020.
2. Rydz, J.; Sikorska, W.; Kyulavska, M.; Christova, D. Polyester-Based (Bio)degradable Polymers as Environmentally Friendly Materials for Sustainable Development. *Int. J. Mol. Sci.* **2014**, *16*, 564–596, doi:10.3390/ijms16010564.
3. Siracusa, V.; Rocculi, P.; Romani, S.; Rosa, M. D. Biodegradable polymers for food packaging: a review. *Trends Food Sci. Technol.* **2008**, *19*, 634–643, doi:10.1016/j.tifs.2008.07.003.
4. Woodruff, M. A.; Hutmacher, D. W. The return of a forgotten polymer—Polycaprolactone in the 21st century. *Prog. Polym. Sci.* **2010**, *35*, 1217–1256, doi:10.1016/j.progpolymsci.2010.04.002.
5. Zhang, C. Biodegradable Polyesters: Synthesis, Properties, Applications. In *Biodegradable Polyesters*; Wiley-VCH Verlag GmbH & Co. KGaA: Weinheim, Germany, 2015; pp. 1–24.
6. Reddy, C. S. .; Ghai, R.; Kalia, V. . Polyhydroxyalkanoates: an overview. *Bioresour. Technol.* **2003**, *87*, 137–146, doi:10.1016/S0960-8524(02)00212-2.
7. Chen, F.-M.; Liu, X. Advancing biomaterials of human origin for tissue engineering. *Prog. Polym. Sci.* **2016**, *53*, 86–168, doi:10.1016/j.progpolymsci.2015.02.004.
8. Tschan, M. J.-L.; Brulé, E.; Haquette, P.; Thomas, C. M. Synthesis of biodegradable polymers from renewable resources. *Polym. Chem.* **2012**, *3*, 836–851, doi:10.1039/C2PY00452F.
9. Nakajima, H.; Dijkstra, P.; Loos, K. The Recent Developments in Biobased Polymers toward General and Engineering Applications: Polymers that are Upgraded from Biodegradable Polymers, Analogous to Petroleum-Derived Polymers, and Newly Developed. *Polymers (Basel).* **2017**, *9*, 523, doi:10.3390/polym9100523.
10. Papageorgiou, G. Thinking Green: Sustainable Polymers from Renewable Resources. *Polymers (Basel).* **2018**, *10*, 952, doi:10.3390/polym10090952.
11. Xu, J.; Guo, B.-H. Poly(butylene succinate) and its copolymers: Research, development and industrialization. *Biotechnol. J.* **2010**, *5*, 1149–1163, doi:10.1002/biot.201000136.
12. Gigli, M.; Fabbri, M.; Lotti, N.; Gamberini, R.; Rimini, B.; Munari, A. Poly(butylene succinate)-based polyesters for biomedical applications: A review. *Eur. Polym. J.* **2016**, *75*, 431–460, doi:10.1016/j.eurpolymj.2016.01.016.
13. Gan, Z.; Abe, H.; Kurokawa, H.; Doi, Y. Solid-state microstructures, thermal properties, and crystallization of biodegradable poly(butylene succinate) (PBS) and its copolyesters. *Biomacromolecules* **2001**, *2*, 605–613, doi:10.1021/bm015535e.
14. Gigli, M.; Negroni, A.; Soccio, M.; Zanaroli, G.; Lotti, N.; Fava, F.; Munari, A. Influence of chemical and architectural modifications on the enzymatic hydrolysis of poly(butylene

succinate). *Green Chem.* **2012**, *14*, 2885, doi:10.1039/c2gc35876j.
15. Liverani, L.; Piegat, A.; Niemczyk, A.; El Fray, M.; Boccaccini, A. R. Electrospun fibers of poly(butylene succinate–co–dilinoleic succinate) and its blend with poly(glycerol sebacate) for soft tissue engineering applications. *Eur. Polym. J.* **2016**, *81*, 295–306, doi:10.1016/j.eurpolymj.2016.06.009.
16. Dai, X.; Qiu, Z. Synthesis and properties of novel biodegradable poly(butylene succinate-co-decamethylene succinate) copolyesters from renewable resources. *Polym. Degrad. Stab.* **2016**, *134*, 305–310, doi:10.1016/j.polymdegradstab.2016.11.004.
17. Tan, B.; Bi, S.; Emery, K.; Sobkowicz, M. J. Bio-based poly(butylene succinate-co-hexamethylene succinate) copolyesters with tunable thermal and mechanical properties. *Eur. Polym. J.* **2017**, *86*, 162–172, doi:10.1016/j.eurpolymj.2016.11.017.
18. Cao, A.; Okamura, T.; Nakayama, K.; Inoue, Y.; Masuda, T. Studies on syntheses and physical properties of biodegradable aliphatic poly(butylene succinate-co-ethylene succinate)s and poly(butylene succinate-co-diethylene glycol succinate)s. *Polym. Degrad. Stab.* **2002**, *78*, 107–117, doi:10.1016/S0141-3910(02)00124-6.
19. Chrissafis, K.; Paraskevopoulos, K. M.; Bikiaris, D. N. Thermal degradation mechanism of poly(ethylene succinate) and poly(butylene succinate): Comparative study. *Thermochim. Acta* **2005**, *435*, 142–150, doi:10.1016/j.tca.2005.05.011.
20. Wang, G.; Qiu, Z. E ff ects of Preexisting Poly(butylene succinate- co -24 mol % hexamethylene succinate) Crystals on the Crystallization Behavior and Crystalline Morphology of Poly(butylene adipate) in Their Melt- Miscible Polymer Blend. **2014**, doi:10.1021/ie403778d.
21. El Fray, M.; Słonecki, J. Multiblock copolymers consisting of polyester and polyaliphatic blocks. *Angew. Makromol. Chem.* **1996**, *234*, 103–117.
22. Kozlowska, A.; Gromadzki, D.; Fray, M. El; Štěpánek, P. Morphology Evaluation of Biodegradable Copolyesters Based on Dimerized Fatty Acid Studied by DSC , SAXS and WAXS. *Fibres Text. East. Eur.* **2008**, *16*, 85–88.
23. Thiele, U. K. Quo vadis polyester catalyst? *Chem. Fibers Int.* **2004**, *54*, 162–163.
24. Pang, K.; Kotek, R.; Tonelli, A. Review of conventional and novel polymerization processes for polyesters. *Prog. Polym. Sci.* **2006**, *31*, 1009–1037, doi:10.1016/J.PROGPOLYMSCI.2006.08.008.
25. Finelli, L.; Lorenzetti, C.; Messori, M.; Sisti, L.; Vannini, M. Comparison between titanium tetrabutoxide and a new commercial titanium dioxide based catalyst used for the synthesis of poly(ethylene terephthalate). *J. Appl. Polym. Sci.* **2004**, *92*, 1887–1892, doi:10.1002/app.20171.
26. Correlo, V. M.; Boesel, L. F.; Bhattacharya, M.; Mano, J. F.; Neves, N. M.; Reis, R. L. Properties of melt processed chitosan and aliphatic polyester blends. *Mater. Sci. Eng. A* **2005**, *403*, 57–68, doi:10.1016/J.MSEA.2005.04.055.
27. Pope, C. G. X-Ray Diffraction and the Bragg Equation. **1997**, *74*, 129–131, doi:10.1021/ed074p129.

28. Solomon, O. F.; Ciută, I. Z. Détermination de la viscosité intrinsèque de solutions de polymères par une simple détermination de la viscosité. *J. Appl. Polym. Sci.* **1962**, *6*, 683–686, doi:10.1002/app.1962.070062414.
29. ISO *Biological evaluation of medical devices—Part 5: tests for in vitro cytotoxicity*; Geneva, Switzerland, 2009;
30. Riss, T. L.; Moravec, R. A.; Niles, A. L.; Duellman, S.; Benink, H. A.; Worzella, T. J.; Minor, L. Cell Viability Assays. In *Assay Guidance Manual*; Sittampalam, G., Coussens, N., Eds.; Eli Lilly & Company and the National Center for Advancing Translational Sciences: Bethesda, MD, 2004.
31. Brostow, W.; Chiu, R.; Kalogeras, I. M.; Vassilikou-Dova, A. Prediction of glass transition temperatures: Binary blends and copolymers. *Mater. Lett.* **2008**, *62*, 3152–3155, doi:10.1016/j.matlet.2008.02.008.
32. Wcisłek, A.; Sonseca Olalla, A.; McClain, A.; Piegat, A.; Sobolewski, P.; Puskas, J.; El Fray, M. Enzymatic Degradation of Poly(butylene succinate) Copolyesters Synthesized with the Use of Candida antarctica Lipase B. *Polymers (Basel).* **2018**, *10*, 688, doi:10.3390/polym10060688.
33. Zhu, P.; Dong, X.; Wang, D. Strain-Induced Crystallization of Segmented Copolymers: Deviation from the Classic Deformation Mechanism. *Macromolecules* **2017**, *50*, 3911–3921, doi:10.1021/acs.macromol.6b02747.
34. Jacquel, N.; Freyermouth, F.; Fenouillot, F.; Rousseau, A.; Pascault, J. P.; Fuertes, P.; Saint-Loup, R. Synthesis and properties of poly(butylene succinate): Efficiency of different transesterification catalysts. *J. Polym. Sci. Part A Polym. Chem.* **2011**, *49*, 5301–5312, doi:10.1002/pola.25009.

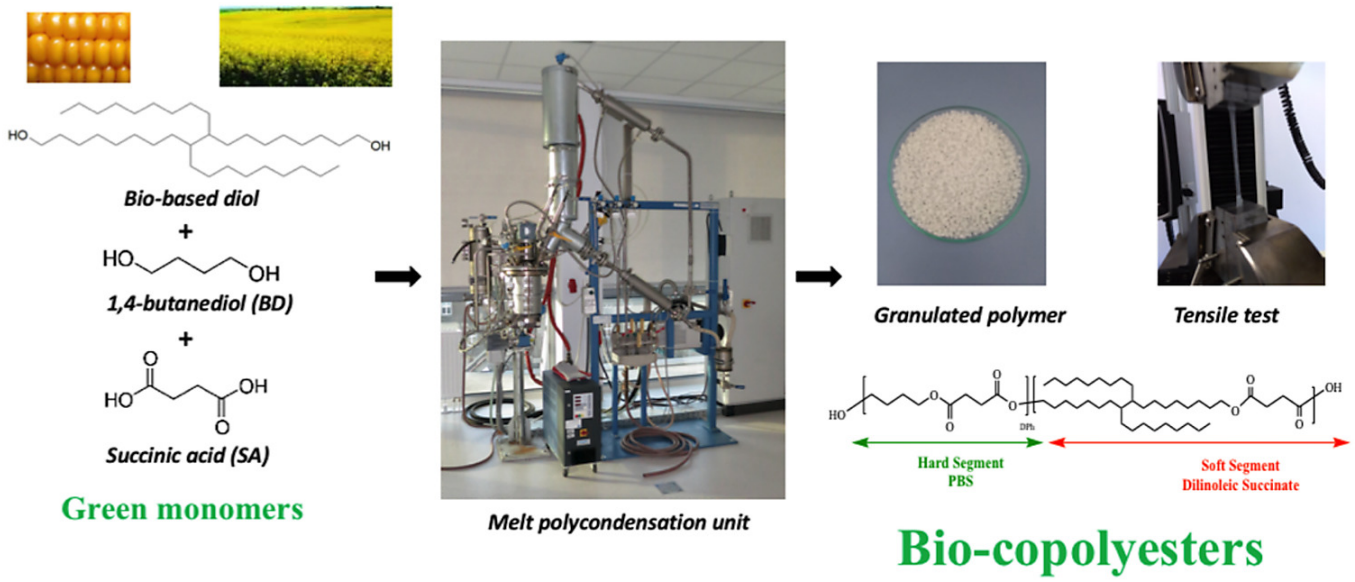

GraphicalAbs.png (739.19 KiB) view on ChemRxiv • download file